Am J Physiol Lung Cell Mol Physiol 306: L162–L169, 2014.
First published November 8, 2013; doi:10.1152/ajplung.00095.2013.

Deletion of airway cilia results in noninflammatory bronchiectasis and hyperreactive airways

Sandra K. Gilley,[1] Antine E. Stenbit,[1] Raymond C. Pasek,[4] Kelli M. Sas,[1] Stacy L. Steele,[1] May Amria,[1] Marlene A. Bunni,[1] Kimberly P. Estell,[4] Lisa M. Schwiebert,[4] Patrick Flume,[1] Monika Gooz,[1] Courtney J. Haycraft,[1] Bradley K. Yoder,[4] Caroline Miller,[3] Jacqueline A. Pavlik,[5] Grant A. Turner,[5] Joseph H. Sisson,[5] and P. Darwin Bell[1,2]

[1]*Department of Medicine, Medical University of South Carolina, Charleston, South Carolina;* [2]*Ralph H. Johnson Veterans Affairs Medical Center, Charleston, South Carolina;* [3]*Department of Anatomy and Cell Biology, Indiana University School of Medicine, Indianapolis, Indiana;* [4]*Department of Cell, Developmental, and Integrative Biology, University of Alabama at Birmingham, Birmingham, Alabama; and* [5]*Pulmonary, Critical Care, Sleep & Allergy Division, Department of Internal Medicine, University of Nebraska Medical Center, Omaha, Nebraska*

Submitted 11 April 2013; accepted in final form 29 October 2013

Gilley SK, Stenbit AE, Pasek RC, Sas KM, Steele SL, Amria M, Bunni MA, Estell KP, Schwiebert LM, Flume P, Gooz M, Haycraft CJ, Yoder BK, Miller C, Pavlik JA, Turner GA, Sisson JH, Bell PD. Deletion of airway cilia results in noninflammatory bronchiectasis and hyperreactive airways. *Am J Physiol Lung Cell Mol Physiol* 306: L162–L169, 2014. First published November 8, 2013; doi:10.1152/ajplung.00095.2013.—The mechanisms for the development of bronchiectasis and airway hyperreactivity have not been fully elucidated. Although genetic, acquired diseases and environmental influences may play a role, it is also possible that motile cilia can influence this disease process. We hypothesized that deletion of a key intraflagellar transport molecule, IFT88, in mature mice causes loss of cilia, resulting in airway remodeling. Airway cilia were deleted by knockout of IFT88, and airway remodeling and pulmonary function were evaluated. In IFT88$^-$ mice there was a substantial loss of airway cilia on respiratory epithelium. Three months after the deletion of cilia, there was clear evidence for bronchial remodeling that was not associated with inflammation or apparent defects in mucus clearance. There was evidence for airway epithelial cell hypertrophy and hyperplasia. IFT88$^-$ mice exhibited increased airway reactivity to a methacholine challenge and decreased ciliary beat frequency in the few remaining cells that possessed cilia. With deletion of respiratory cilia there was a marked increase in the number of club cells as seen by scanning electron microscopy. We suggest that airway remodeling may be exacerbated by the presence of club cells, since these cells are involved in airway repair. Club cells may be prevented from differentiating into respiratory epithelial cells because of a lack of IFT88 protein that is necessary to form a single nonmotile cilium. This monocilium is a prerequisite for these progenitor cells to transition into respiratory epithelial cells. In conclusion, motile cilia may play an important role in controlling airway structure and function.

bronchiectasis; hyperreactivity; lung; respiratory

MOTILE CILIA IN THE RESPIRATORY airways function in mucus clearance but may also have other mechanosensory and chemical-detection functions (32, 33). In humans, diseases such as primary ciliary dyskinesia (PCD) have led to insights into the consequences of a loss in motile cilia function (36). In some forms of PCD, cilia are present but do not move. One manifestation of PCD is bronchiectasis, a dilation of the lower respiratory airways in lung. In humans, the etiology of bronchiectasis is multifactorial and can range from the consequence of a systemic illness to the manifestation of a genetic abnormality such as cystic fibrosis or immune deficiencies (5, 6). The most widely accepted model for the development of bronchiectasis is the "vicious cycle hypothesis," in which an environmental insult in a genetically susceptible individual leads to impaired mucociliary clearance and persistent microbial colonization with chronic inflammation (6).

In bronchiectasis, as well as other lung diseases such as asthma, there is hyperreactivity of airways (21). In this regard, a study of six patients with ciliary dyskinesia reported airway hyperreactivity to the aerosol administration of methacholine, an agent that activates muscarinic acetylcholine receptors in airways (10). In humans, dilation and hyperreactive airways are usually detected after establishment of bronchiectasis and the development of symptoms; thus, little is known regarding the initiation and initial progression of these pathophysiological conditions. It is also not known if bronchiectasis and hyperreactivity are solely the result of inflammation or could result through some other mechanisms, such as the loss of structure and function of cilia.

Recently, an association between bronchiectasis and polycystic kidney disease (PKD) in humans has been reported (9). PKD is a "ciliopathic" disorder that involves the mutation of proteins that are necessary for the structure and function of nonmotile cilia in renal epithelial cells (4). One murine model of PKD involves the deletion of the gene *Ift88*, which encodes for the protein polaris, now called IFT88, an integral component of the intraflagellar transport machinery (34). Although complete loss of IFT88 is embryonic lethal, a mouse that is hypomorph for the *Ift88* (Tg737^{orpk}) gene has severely stunted, nonmotile cilia, massive renal cyst development, a variety of structural and functional abnormalities, and dies shortly after birth. In addition, we previously reported reduced abundance and function of motile cilia in the brain ependyma and choroid plexus, which leads to hydrocephalus, suggesting that IFT88 is also involved in intraflagellar transport and maintenance of motile cilia (2). A conditional floxed allele mouse has recently been developed (14) that allows for global deletion of IFT88 using an inducible cre/lox system (31). IFT88 can be deleted in fully formed adult mice, thereby eliminating the severe developmental abnormalities that occur when cilia are absent in

Address for reprint requests and other correspondence: P. Darwin Bell, 70 President St, DDB520, MUSC, Charleston, SC 29425 (e-mail: Bellpd@musc.edu).

utero. Because IFT88 is also expressed in motile airway cilia (34), this allowed us to determine if deletion of IFT88 would alter the structure and function of airway motile cilia and, if so, to determine if there are pathogenic consequences with the loss of airway cilia.

MATERIALS AND METHODS

Ift88 floxed mouse. The cre$^+$ and cre$^-$ *Ift88* floxed allele mice have been previously reported (8, 14); these mice were maintained in accordance with both the Institutional Animal Care and Use Committee regulations at the Medical University of South Carolina, the University of Alabama at Birmingham (UAB), and the National Institutes of Health Guidelines. Tamoxifen was administered 3 times in 1 week with at least 24 h between injections in both male and female cre$^+$ and cre$^-$ mice at ~8 wk of age. Tamoxifen (Sigma, St. Louis, MO) dissolved in corn oil (Sigma) was administered intraperitoneally (0.5 ml of 10 mg/ml tamoxifen).

Computer tomography imaging of lung. High spatial and temporal resolution (100 μm on-a-side cubic voxels and 50 ms acquisition time, respectively), respiratory-gated micro-computer tomography (CT) images were obtained using a Siemens Inveon Micro-CT scanner (Siemens Medical Solutions, Knoxville, TN) from mice under 2% isoflurane anesthesia. Projection data were acquired, and images were reconstructed using the Siemens software package IRW, implementing the modified Feldkamp reconstruction algorithm.

Tissue preparation. Mice were anesthetized and exsanguinated, and lungs were inflated with a small amount of air. Lungs were perfused with an isotonic phosphate buffer solution (PBS) via cardiac puncture, followed by a 4% paraformaldehyde solution and then incubated in increasing concentrations of sucrose (10, 20, and 30%).

Immunofluorescence. Paraffin-embedded lung tissue sections (5 μm) were processed using traditional immunofluorescence protocols and incubated with primary antibodies against acetylated α-tubulin (Abcam, Cambridge, MA), and IFT88 (Protein Tech, Chicago, IL) or club cell secretory protein (uteroglobin) (Abcam).

Histology. Tissue sections were stained with hematoxylin-eosin (H&E), Masson trichrome, periodic acid-Schiff (PAS) or Alcian Blue. The number of cells per micrometer airway surface and the height of the epithelial cells were assessed by blinded morphometric measurements. Airway diameters were measured relative to the diameter of the adjacent artery.

Western blot. Mouse lung tissue was homogenized at 4°C using a mini bead beater from Biospec (Bartlesville, OK), and proteins were extracted using Thermo Scientific's T-PER Tissue Protein Extraction Reagent (Rockford, IL) containing Halt Protease and Phosphatase Inhibitor Cocktail. Samples (~40 μg protein) were reduced with Tris(2-carboxyethyl)phosphine (Thermo Scientific), and proteins were separated by SDS-PAGE on Tris-glycine gels (Bio-Rad). Proteins were transferred to nitrocellulose using the Life Technologies iBlot (Carlsbad, CA) and immunoblotted with anti-IFT88 (polaris) antibody (1:5,000; gift from Bradley Yoder at UAB). All membranes were blocked in 5% nonfat milk. Immunoblots were visualized using ECL plus (GE Healthcare, Piscataway, NJ) on a Carestream GL2200 Pro imager (Rochester, NY).

Airway reactivity. Mice were mechanically ventilated and exposed to increasing concentrations of methacholine as described previously (16). Total respiratory system resistance was measured continuously as previously described (15). Increasing concentrations of methacholine chloride (0–50 mg/ml; Sigma-Aldrich) were administered via aerosolization. Airway responsiveness was recorded every 15 s for 3 min after each aerosol challenge. Broadband perturbation was used, and impedance was analyzed via a constant-phase model.

Electron microscopy. Lung tissue was processed for electron microscopy using conventional techniques (25). For transmission electron microscopy, thin sections (80 nm) were stained with uranyl actetate and viewed on a Tecnai BioTwin (FEI, Hillsboro, OR). Digital images were taken with an AMT (Advanced Microscope Techniques, Danvers, MA) CCD camera. For scanning electron microscopy (SEM), lung tissue was viewed, and images were taken on a JEOL 6390LV (Peabody, MA) scanning electron microscope.

Ciliary beat frequency and motile points analysis. Tracheas were isolated and placed in media at 4°C. Tracheas were sliced into 1-mm-thick rings and placed into M199 media (GIBCO) supplemented with 10% FBS (GIBCO) and maintained in a 37°C incubator with 5% CO_2. Tracheal ring ciliary beat frequency (CBF) was measured using the Sisson Ammons Video Analysis SAVA system. Experiments were captured as previously described (39). Temperature was maintained at 25°C, controlled by a thermostatic stage. The sampling rate was set at 85 frames/s for all experimental conditions. A minimum number of four separate fields was captured, analyzed, and expressed as mean ± SE for each CBF data point. Significance for paired samples was determined using the Student's *t*-test with a P value <0.05. Significance for more than two conditions was determined using a one-way ANOVA with a P value <0.05.

Motile points and measurement of trachea. Images from SAVA were reconstructed to make each trachea ring with a minimum of nine separate aligned images. The ring images were measured with the Image-Pro Plus Software (Media Cybernetics). To assess micron length of the tracheal rings, three separate measurements for each image were averaged.

Statistical analysis. Nonpaired Student's *t*-test was used for morphometric analysis, and linear regression analysis was used for airway reactivity, using GraphPad software (La Jolla, CA). Significance was denoted as $P < 0.05$.

RESULTS

We hypothesized that conditional deletion of a key intraflagellar transport molecule, IFT88, in mature mice would cause airway remodeling and ciliary dysfunction. To test this hypothesis, 8-wk-old male and female *Ift88* conditional floxed allele mice that express a tamoxifen-inducible form of Cre recombinase under the control of a ubiquitous promoter, cre$^+$, or do not express Cre recombinase, cre$^-$, were injected with tamoxifen and analyzed at either 3 wk or 3 mo posttamoxifen. Previous reports suggest that the cre$^+$ mice have ~80% reduction in IFT88 protein expression 2–3 wk after tamoxifen administration (3, 34); these mice are designated as IFT88$^-$ mice. Tamoxifen administration in cre$^-$ does not affect IFT88 protein abundance and are designed as IFT88$^+$ mice. At either 3 wk or 3 mo posttamoxifen, all mice appeared to be healthy.

Knockout of Ift88 leads to decreased lung IFT88 protein and loss of motile cilia. As shown in Fig. 1, *A* and *C*, in IFT88$^+$ mice there was a normal pattern of motile cilia in respiratory epithelial cells as well as the presence of IFT88. However, there was a dramatic loss of motile cilia in respiratory airways when IFT88 was knocked out in mice at either 3 wk (Fig. 1, *B* and *D*) or at 3 mo (data not shown). Knockout of IFT88 was confirmed by Western blot analysis (Fig. 1, *E* and *F*) in which there was an overall reduction in lung IFT88 of ~70%. As expected, there was some persistent expression of IFT88 in the knockout mice, since it is typically found that a small subpopulation of CreER-expressing cells do not activate the reporter protein (13).

Airway dilation and histological changes in respiratory epithelium. Airway to adjacent artery was used to determine if there were enlarged airways in IFT88$^-$ lungs using H&E-stained tissue preparations (Fig. 2*A*). In the 3 wk mice, the ratio of airway to adjacent artery diameter of the IFT88$^-$ mice was not statistically different from IFT88$^+$ mice. However, there

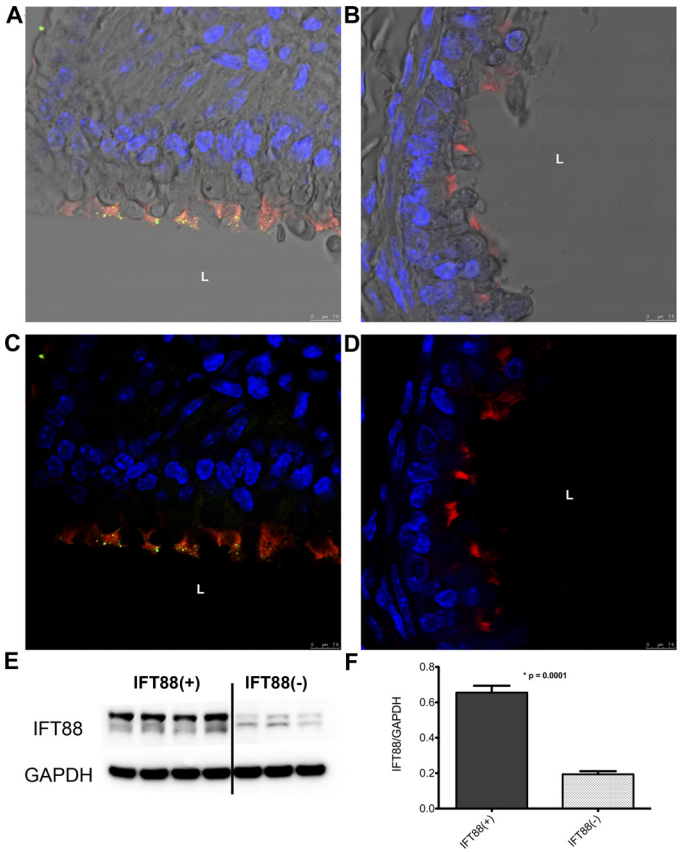

Fig. 1. Representative immunofluorescence (IF) image of lung from an IFT88$^+$ mouse shows ciliated respiratory epithelial cells of a large airway labeled with anti-acetylated α-tubulin (red) and IFT88 (green) colocalization of these two proteins (yellow). Nuclei are stained blue with DAPI (*A* and *C*). Compared with the IFT88$^+$ mice ($n = 7$) that expressed abundant cilia, there is a marked loss of cilia in both the 3 wk ($n = 5$) (*B* and *D*) and 3 mo ($n = 3$; data not shown) *Ift88* knockout animals. *A* and *B* show brightfield illumination in addition to fluorescence. Western blot analysis from lung confirms 70% reduction of lung IFT88 (*E* and *F*). Scale bars represent 7.5 μm.

were some instances (Fig. 2*A*, *middle*) where airways were clearly dilated in the 3 wk IFT88$^-$ mouse. In 3 mo mice, the ratio of airway to adjacent artery diameter of the IFT88$^-$ mice was significantly different from IFT88$^+$ mice. Because airway-to-artery diameter is relatively consistent along the respiratory tree (17), comparison of IFT88$^-$ to IFT88$^+$ ratios is independent of the airway segment that is being measured. Thus, there was significant bronchiectasis at 3 mo in lungs that lacked IFT88 and cilia. This was confirmed using in vivo CT imaging (Fig. 2*B*). Although there was a tendency for dilated airways in 3 wk IFT88$^-$ mice (images not shown), pronounced airway dilation was observed at 3 mo in IFT88$^-$ mice on CT scan. All visible airways of the IFT88$^-$ mice appeared to be larger than the comparable airways of IFT88$^+$ mice (Fig. 2*B*).

Histological characteristics of the IFT88$^-$ mouse lung. As shown in Fig. 3, *A* and *B*, there was hypertrophy of airway epithelial cells, with increased cytoplasmic blebbing in airways from IFT88$^-$ mice. Morphological measurements of cell height and cell number (Fig. 3*B*) substantiated both significant air epithelial cell hypertrophy as well as cell proliferation in both 3 wk and 3 mo IFT88$^-$ vs. IFT88$^+$ mice. TUNEL assay revealed no apparent increase in the number of apoptotic cells in the IFT88$^-$ mice at either 3 wk or 3 mo (data not shown).

As shown in Fig. 4*A*, there was no apparent change in glycogen content; however, PAS staining showed the presence of some macrophages in lung parenchyma of the IFT88$^-$ mice, especially at 3 mo (Fig. 4*B*). Masson trichrome staining was used to determine if there were changes in basement membrane or connective tissue abundance in this model (Fig. 4*C*). As shown in Fig. 4*C*, there was minimal increase in bronchial wall thickness and little evidence for increased connective tissue in lungs from 3 wk or 3 mo IFT88$^-$ mice. Thus, there was little evidence for an overt inflammatory response with deletion of cilia.

Alcian blue staining did not demonstrate an increase in the number of goblet cells (Fig. 5*A*), and there did not appear to be a detectable difference in the amount of mucus that lined the airways of IFT88$^+$ or IFT88$^-$ mice.

Club cells. Certain morphological characteristics of the respiratory epithelial cells in the absence of cilia led us to determine if there might be an increase in the number of club cells within the respiratory bronchioles (28, 37). As shown in Fig. 6, *A–C*, SEM demonstrated a marked loss of cilia in the large airways of IFT88$^-$ mice and the presence of cells that resemble club cells (27, 37). Although we recognize that the cellular constituents normally vary along the respiratory tract (30), in IFT88$^-$ mice the vast majority of respiratory epithelial cells in both large and small airways had the "dome-like" appearance that is characteristic of club cells. The increase in club cell number was confirmed by counting club cells (Fig. 6*F*), and the presence of club cells was confirmed by staining for club cell secretory protein (Fig. 6*E*).

Airway hyperreactivity. Standard methacholine challenge was used to determine if IFT88$^-$ mice had hyperreactive airways. Results are shown in Fig. 7. There was a significant increase in airway reactivity at 3 mo in mice that lacked IFT88 compared with mice that had IFT88. Interestingly, in IFT88$^-$ mice, two mice in the 3 wk group and three mice in the 3 mo group had starting resistances in the range of 5–7 $cmH_2O \cdot ml^{-1} \cdot s^{-1}$ and failed to respond to methacholine. These mice were not included in the analysis shown in Fig. 7.

Motility points and CBF. Isolated trachea rings were examined for the presence of functional motile cilia and to assess CBF. As shown in Fig. 8, using SAVA analysis with high-speed imaging, there were significantly fewer motility points, and thus much less motile cilia in the IFT88$^-$ mice compared with the IFT88$^+$ mouse trachea. Interestingly, CBF was likewise lower in those few cilia that remain in the IFT88$^-$ compared with the IFT88$^+$.

DISCUSSION

The impetus for these studies was the clinical observation that patients with PKD have an increased frequency of bronchiectasis (9). This finding led us to hypothesize that there is a link between cilia and the development of bronchiectasis. To test this hypothesis we used a PKD mouse model in which IFT88, an essential component of intraflagellar transport, was knocked out in the adult mouse (3, 7, 14). Elimination of IFT88 resulted in a loss of airway cilia in lung, suggesting that IFT88 is essential for maintaining cilia along the respiratory tract. Loss of cilia was found throughout airways and tracheal epithelial cells. These finding were not surprising since a mouse hypomorph of *Ift88* exhibits loss of motile cilia in

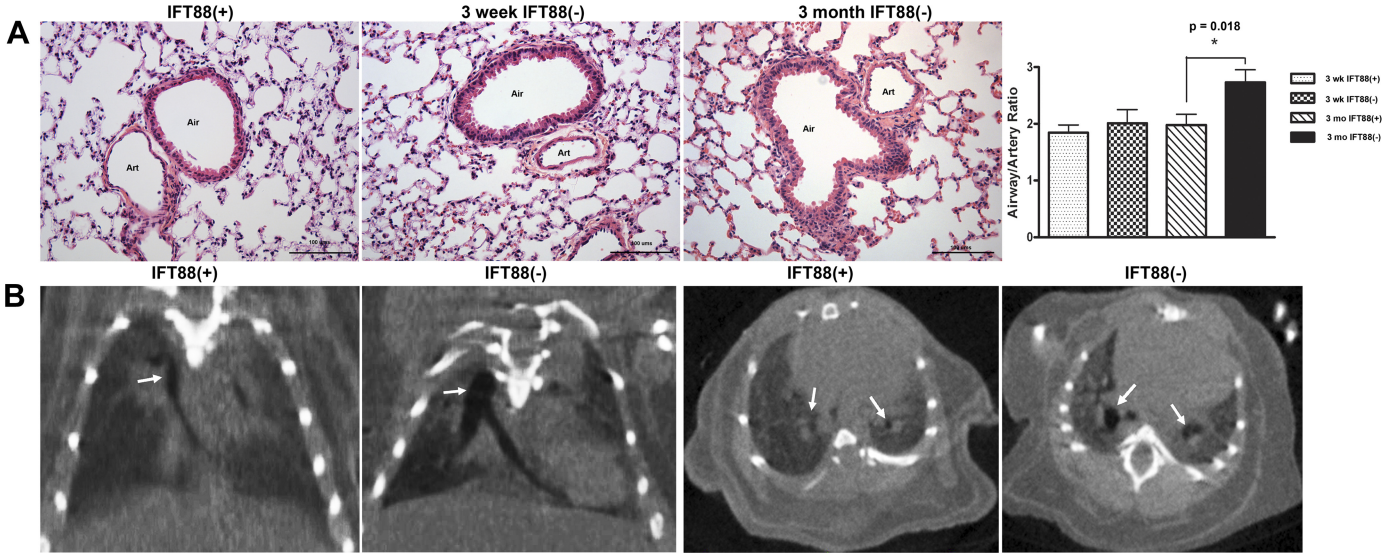

Fig. 2. *A*: hematoxylin-eosin (H&E) staining demonstrates that airways of the IFT88$^-$ mice (*middle* and *right*) have a greater diameter than that of the adjacent artery compared with the IFT88$^+$ mice (*left*), which have airway diameters that approximate that of the adjacent vessel. Airway-to-vessel ratios are summarized. While we did observe some dilated airways in the 3 wk animals (*middle* image in *A*), the ratios for the group as a whole are not significantly different from the IFT88$^+$ group; however, at 3 mo, there was a highly significant enlargement of airway diameter in the IFT88$^-$ group. Computer tomography (CT) scans were obtained from IFT88$^+$ ($n = 3$) and 3 mo IFT88$^-$ ($n = 6$) lungs in anesthetized mice. Airways of the IFT88$^-$ mouse (*B*) are dilated compared with airways of the control group (arrows denote airways).

ependyma and choroid plexus, which leads to hydrocephalus (2). We report that loss of airway cilia, due to knockout of IFT88, causes structural and functional abnormalities in airways, resulting in noninflammatory bronchiectasis and airway hyperreactivity.

Development of bronchiectasis does not appear to involve impaired mucociliary clearance. There was no change in the number of goblet cells nor were there detectable changes in respiratory mucus secretions in the IFT88$^-$ mice. Given the paucity of cilia and the fact that what cilia remained beat slower than cilia from IFT88$^+$ mice, it is difficult to understand how mucociliary clearance could be completely normal. There was, however, no evidence of mucus plugging either by CT or histology. A note of caution is the possibility that conditions in which the lungs were processed for histology may have altered mucus secretions or plugs. However, the distribution of bronchiectasis on CT appeared to be diffuse, as opposed to the localized bronchiectasis that is usually seen with retained secretions (20). In contrast to humans, previous mouse models of PCD have not shown lower airway pathology. Ostrowski et al. noted impaired mucociliary clearance in the nasopharynx of conditional knockouts of *Dnaic 1*, but normal mucociliary clearance in the lower airways for up to 6 mo (26). These findings may be because of alternative mechanisms of muco-

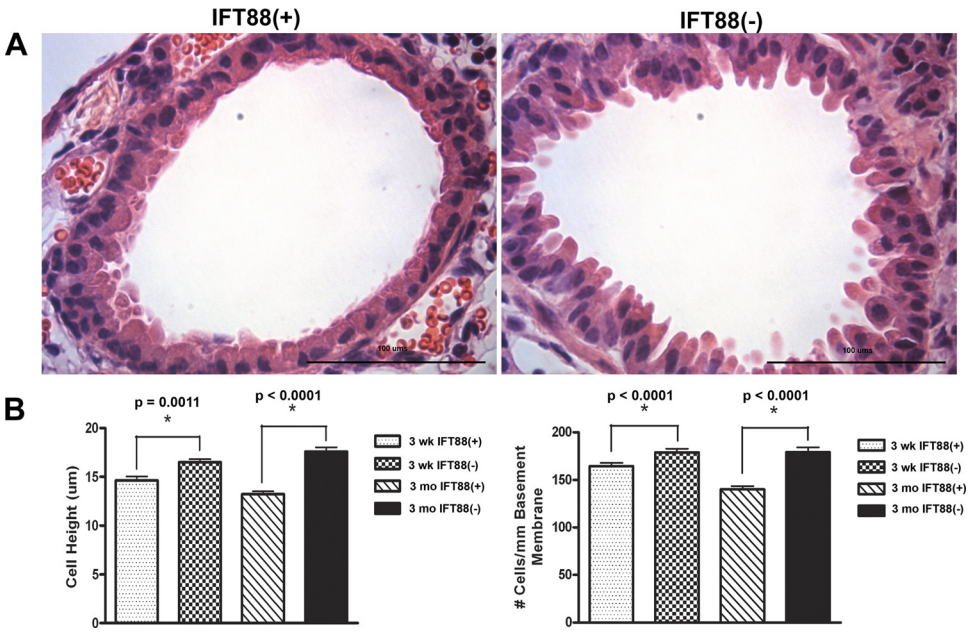

Fig. 3. As shown in *A*, there is hypertrophy of airway cells with increased cytoplasmic blebbing in IFT88$^-$ but not IFT88$^+$ mice. *B*: summary of cell height measurements of epithelial cells lining airways. IFT88$^-$ cell heights are significantly increased. Also shown in *B*, *right*, there is increased cell proliferation in 3 wk and 3 mo respiratory epithelial cells as assessed by the no. of cells per area of basement membrane. Note: representative images and measurements for Figs. 2–5 were obtained from the following groups: IFT88$^+$ mice, $n = 5$ (3 wk), $n = 4$ (3 mo) and for the IFT88$^-$ mice, $n = 5$ (3 wk), $n = 3$ (3 mo).

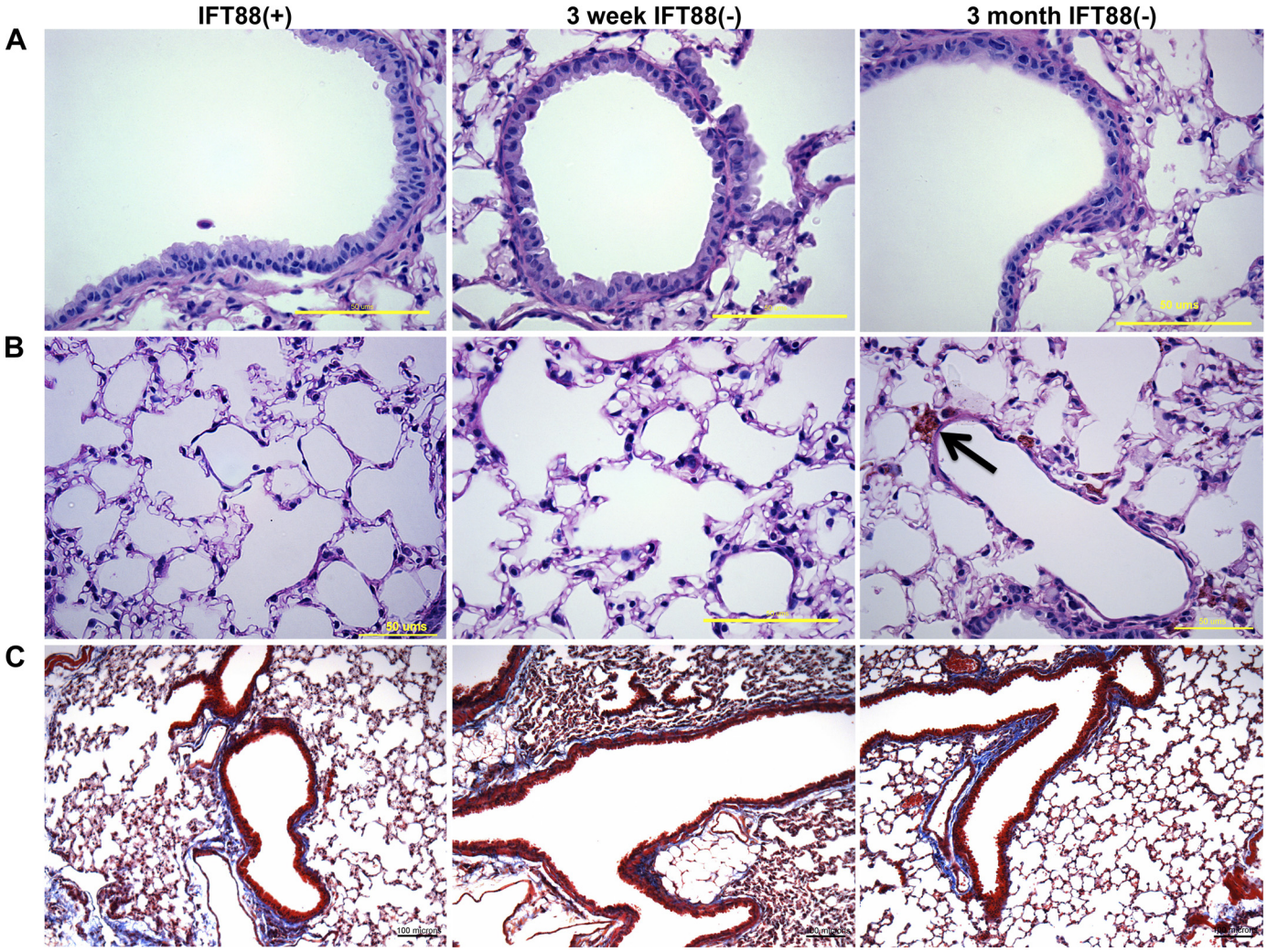

Fig. 4. *A* and *B*: periodic acid-Schiff (PAS) stain of lung tissue demonstrates the presence of alveolar macrophages (*B*, *right*, arrow) present in the 3 mo IFT88^{-} mice but no peribronchiolar inflammation in IFT88^{-} mice at 3 wk or 3 mo. *C*: Masson trichrome staining demonstrates a minimal increase in connective tissue (blue staining) around the bronchial wall. The yellow scale bars represent 50 μm.

ciliary clearance in the lower airways of mice. In another model, mice with knockout of the ciliary structural protein Chibby (Cby) have a paucity of cilia in both the upper and lower airways but seem to have normal clearance of bacteria from the lower airways despite having impaired nasopharyngeal mucociliary transport, leading to severe sinusitis and otitis (23, 35). The mice in the Cby model have also been reported to have enlarged airways, consistent with the present studies.

The mouse lung appears to be relatively resistant to many of the genetic, infective, and environmental insults that cause symptomatic disease and altered lung structure and function in humans. For instance, the Δ508-mutation in cystic fibrosis transmembrane conductance regulator does not lead to cystic fibrosis in the mouse (11), which may be related to differences in airway sodium channel function in mice compared with humans. In the knockouts of *Dnaic 1* and in

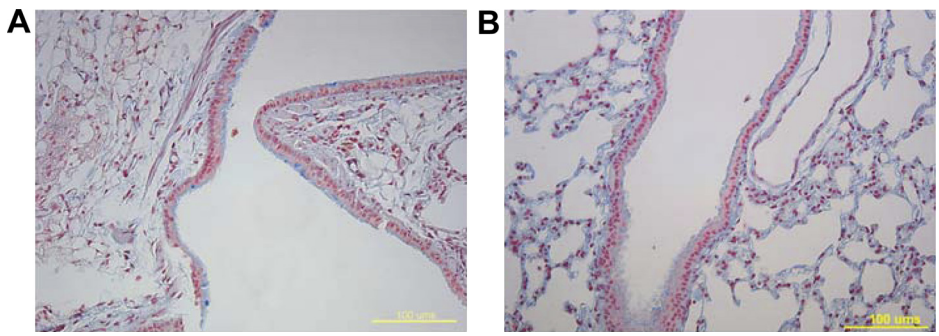

Fig. 5. Alcian blue staining does not demonstrate an increase in the no. of goblet cells or mucus production between IFT88^{+} (*A*) and IFT88^{-} (*B*) mice. The yellow scale bars represent 100 μm.

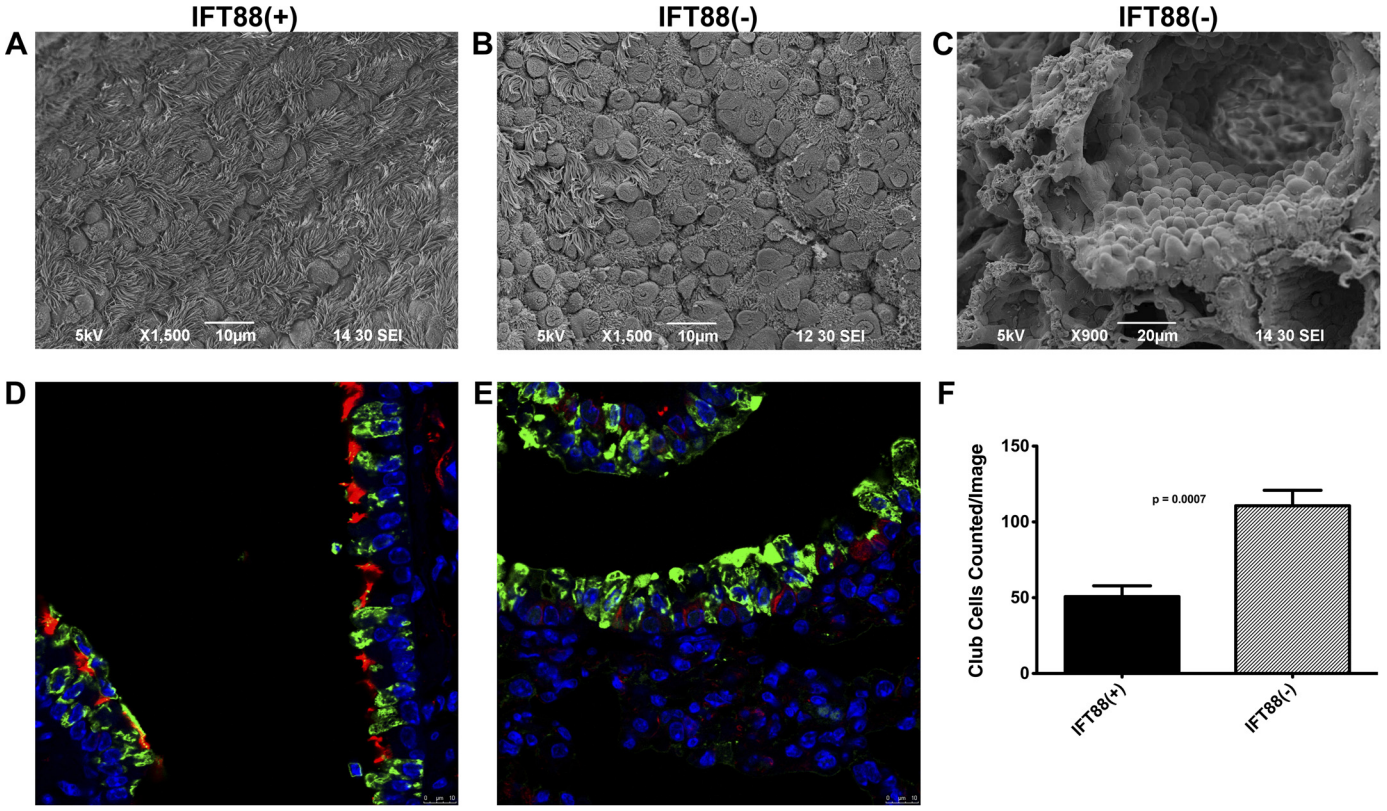

Fig. 6. *A–C*: representative scanning electron micrographs that demonstrate a marked loss of cilia in the large airways of the IFT88$^-$ mice ($n = 4$) vs. IFT88$^+$ mice ($n = 4$) at 3 mo. To quantify the increase in club cells, these cells were manually counted in scanning electron microscopy (SEM) images taken at ×1,500 using ImageJ's Cell Counter. GraphPad was used to perform unpaired Student's *t*-test between IFT88$^+$ and IFT88$^-$ cell counts, and, as shown in *F*, there were significantly more club cells in the IFT88$^-$ images. Club cells were identified in *D* and *E* by staining for club cell secretory protein (green) with anti-acetylated α-tubulin in red. Scale bars in IF images represent 10 μm.

other mouse models of PCD, cilia are still present but are not motile, indicating that cilia immotility may not be sufficient to cause significant airway pathology. For instance, TRPV4 (22), polycystin 1, polycystin 2 (1), and other proteins involved in signaling pathways are located in cilia and participate in regulating CBF (18) and airway surface liquid composition. It may be that these pathways remain intact in cilia with impaired motility (models of PCD) and thus maintain at least some cilia-dependent functional activity. The finding that loss of respiratory ciliary motility in mice in some cases does not lead to lung pathology, whereas elimination of cilia on the respiratory epithelium leads to bronchiectasis, may provide novel insights into the initiation and development of bronchiectasis.

In the kidney, the loss of cilia in the IFT88 knockout mouse affects numerous signaling pathways, including activation of the mitogen-activated protein kinase pathway, leading to cellular hypertrophy and hyperplasia and resulting in cyst formation (3). We observed that there was cell hypertrophy and possible increased cell proliferation without increased apopto-

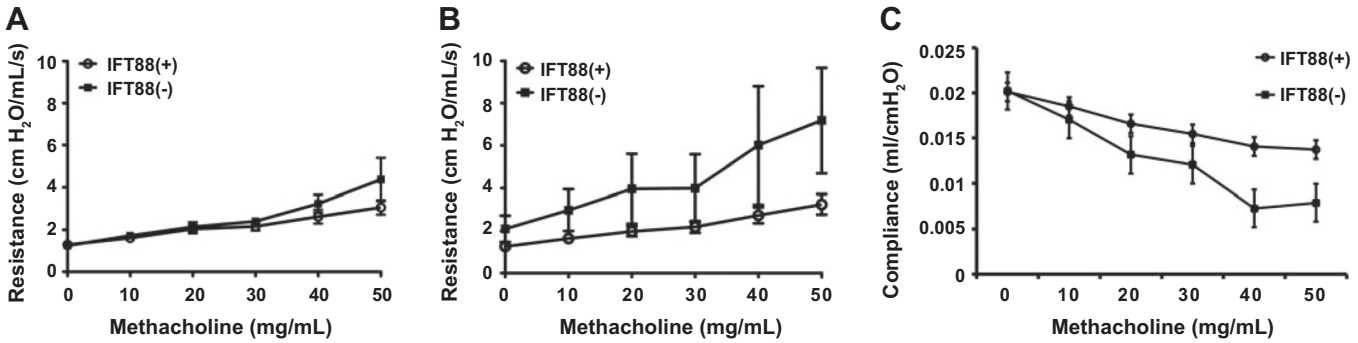

Fig. 7. *A–C*: airway resistance was measured in the absence of and in the presence of increasing concentrations of inhaled methacholine. Linear regression analysis, using GraphPad software, showed that, at 3 wk (*A*), the slopes of the airway resistance to methacholine were not significantly different; however, at 3 mo (*B*), the slopes of the airway resistance to methacholine were significantly different between the IFT88$^-$ and IFT88$^+$ mice ($P < 0.0001$ for 3 mo groups). Also at 3 mo, the calculated compliance, as shown in *C*, was decreased in response to a methacholine challenge, as expected. At 3 wk there were $n = 4$ IFT88$^-$ and $n = 8$ IFT88$^+$ mice and at 3 mo there were $n = 10$ IFT88$^-$ and $n = 12$ IFT88$^+$ mice.

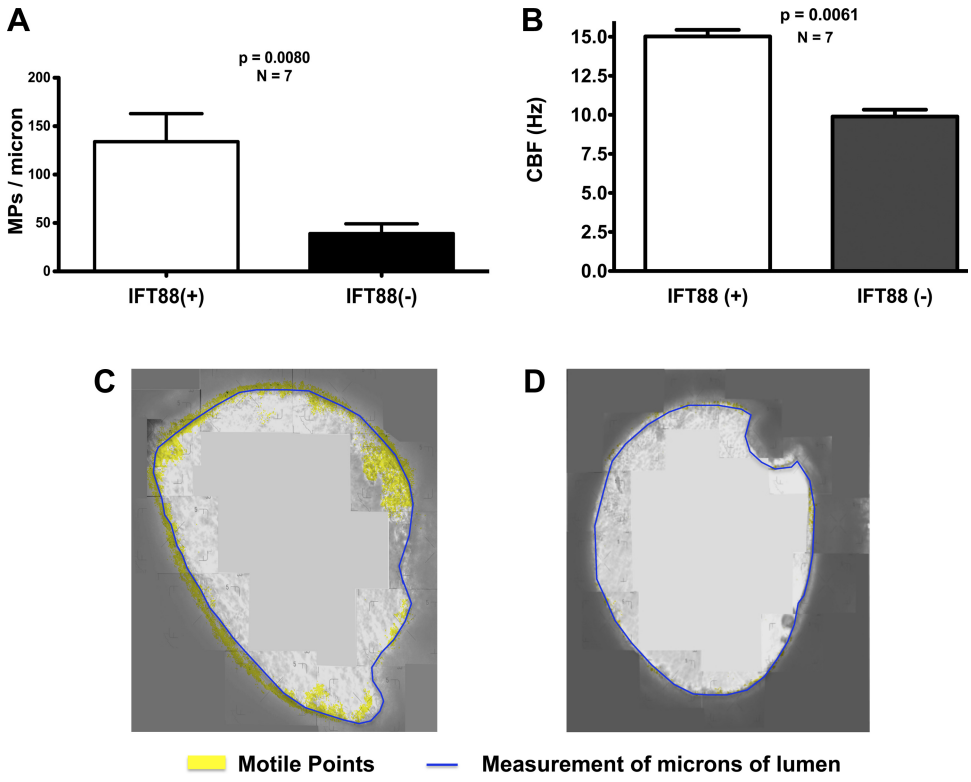

Fig. 8. *A–C*: measurements of motility points and ciliary beat frequency (CBF) in isolated trachea from 3 mo mice using the SAVA system with optical imaging. Measurements were obtained in $n = 8$ IFT88$^+$ and $n = 8$ IFT88$^-$ mice. *A* shows the calculated motility points that were obtained from such images as shown in *C*, where yellow represents motile cilia, whereas in *D* there is little motile cilia in the trachea from the IFT88$^-$ mouse. In those motile cilia that remained in IFT88$^-$ trachea, there was a clear decrease in CBF (*B*).

sis in airway epithelial cells in the IFT88$^-$ mice. We speculate that the cellular hypertrophy and hyperplasia found in airways of the IFT88$^-$ mice maybe the result of mechanisms that are similar to those that occur in renal epithelial cells. Alternatively, the increased cell height and cell number may reflect the preponderance of club cells that line the respiratory tract in the IFT88$^-$ mice. It has been reported that the Cby model has decreased cell proliferation (23). However, Cby knockout occurs embryonically, so there may be substantial differences in the effects of cilia knockout in utero vs. in the adult animal. This is true in kidney where there are dramatic differences in the rate of cyst formation with embryonic vs. adult knockout of cilia (14). Airway smooth muscle cells, which possess nonmotile cilia, are also involved in the airway maintenance, remodeling, and injury repair. Loss of primary cilia on airway smooth muscle cells causes changes in migration in cell culture scratch wound assay (24, 38). Impaired smooth muscle cell migration is perhaps another component in the pathogenesis of bronchiectasis.

Mice lacking cilia demonstrated hyperreactivity to a methacholine challenge. At the present time, the mechanism(s) that result in hyperreactivity are unknown, although hyperreactivity has been shown to occur in bronchiectasis. It is possible that increased airway resistance with methacholine could involve altered signaling from the respiratory epithelium to the smooth muscle cells or changes in the contractility of the airway smooth muscle cells. Thus, our data suggest that loss of cilia structure and function can influence airway reactivity, and this provides a new and perhaps important pathway to understanding the mechanisms that control airway reactivity.

Club cells are facultative progenitor cells for airway epithelium (28). Injury to the epithelium activates and leads to club cell-mediated repair and the eventual differentiation of club cells into terminally differentiated respiratory epithelial ciliated cells or mucus cells. We observed a dramatic increase in the percentage of club cells in airways of IFT88$^-$ mice. As shown by Jain et al. (19), development of respiratory epithelial cells from progenitor cells is dependent upon the development of a single primary nonmotile cilia followed by the development of multiple motile cilia. Thus, the lack of an intact, functional intraflagellar transport system prevents the formation of primary cilia and therefore prevents club cells from differentiating into respiratory epithelium. We speculate that the excessive number of club cells in airways of the *Ift88* knockout mice leads to an ongoing process of "repair and remodeling" of the respiratory tract. Presumably, over time this continuous remodeling process leads to dilation of the airways and the condition that is defined as bronchiectasis. Because there was no insult or injury other than genetically induced loss of cilia, this would suggest that either cilia loss per se or the inability to generate new cilia might be a stimulus for club cell proliferation. This is an interesting concept since adenocarcinoma of the lung may originate from club cells (12).

In conclusion we report that conditional deletion of motile cilia in the lung of the adult mouse results in the development of bronchiectasis, slower cilia, and increased airway hyperreactivity. Our findings suggest that loss of cilia leads to morphological changes of airway epithelial cells with cellular hyperplasia and proliferation of club cells, leading to airway dilation. Understanding the pathophysiology of the early stages of bronchiectasis has been limited by the lack of a suitable animal model. This mouse model may serve as a means for defining the role of cilia in the pathophysiological response of the lung to infection, asthma, and exposure to toxins, as well as the maintenance of airway homeostasis.

ACKNOWLEGMENTS

We thank the University of Alabama at Birmingham (UAB) Polycystic Kidney Disease (PKD) Recessive Core Facility for help with this project. In addition, we thank Dr. Vincent Gattone II and the PKD Foundation Electron Microscopy Core for the electron micrographs.

GRANTS

This project was supported by a Veterans Affairs Merit Grant (P. D. Bell), Core C of the UAB P30-DK-074038, DK-32032 (P. D. Bell), DK-065655 (B. K. Yoder), RO1-AA-008769 (J. H. Sisson), and funds from Dialysis Clinic.

DISCLOSURES

No conflicts of interest, financial or otherwise are declared by the authors.

AUTHOR CONTRIBUTIONS

Author contributions: S.K.G., A.E.S., L.M.S., and P.D.B. conception and design of research; S.K.G., A.E.S., R.C.P., S.L.S., M.A., M.A.B., K.P.E., M.G., C.M., J.A.P., G.A.T., and P.D.B. performed experiments; S.K.G., A.E.S., R.C.P., K.M.S., S.L.S., M.A.B., L.M.S., M.G., and P.D.B. analyzed data; S.K.G., A.E.S., R.C.P., K.M.S., P.F., C.J.H., B.K.Y., J.H.S., and P.D.B. interpreted results of experiments; S.K.G., A.E.S., and P.D.B. drafted manuscript; S.K.G., A.E.S., S.L.S., J.H.S., and P.D.B. edited and revised manuscript; S.L.S., J.A.P., and P.D.B. prepared figures; P.D.B. approved final version of manuscript.

REFERENCES

1. **AbouAlaiwi WA, Takahashi M, Mell BR, Jones TJ, Ratnam S, Kolb RJ, Nauli SM.** Ciliary polycystin-2 is a mechanosensitive calcium channel involved in nitric oxide signaling cascades. *Circ Res* 104: 860–869, 2009.
2. **Banizs B, Pike MM, Millican CL, Ferguson WB, Komlosi P, Sheetz J, Bell PD, Schwiebert EM, Yoder BK.** Dysfunctional cilia lead to altered ependyma and choroid plexus function, and result in the formation of hydrocephalus. *Development* 132: 5329–5339, 2005.
3. **Bell PD, Fitzgibbon W, Sas K, Stenbit AE, Amria M, Houston A, Reichert R, Gilley S, Siegal GP, Bissler J, Bilgen M, Chou PC, Guay-Woodford L, Yoder B, Haycraft CJ, Siroky B.** Loss of primary cilia upregulates renal hypertrophic signaling and promotes cystogenesis. *J Am Soc Nephrol* 22: 839–848, 2011.
4. **Chapin HC, Caplan MJ.** The cell biology of polycystic kidney disease. *J Cell Biol* 191: 701–710, 2010.
5. **Cohen M, Sahn SA.** Bronchiectasis in systemic diseases. *Chest* 116: 1063–1074, 1999.
6. **Cole PJ.** Inflammation: a two-edged sword–the model of bronchiectasis. *Eur J Respir Dis Suppl* 147: 6–15, 1986.
7. **Davenport JR, Watts AJ, Roper VC, Croyle MJ, van Groen T, Wyss JM, Nagy TR, Kesterson RA, Yoder BK.** Disruption of intraflagellar transport in adult mice leads to obesity and slow-onset cystic kidney disease. *Curr Biol* 17: 1586–1594, 2007.
8. **Davenport JR, Watts AJ, Roper VC, Croyle MJ, van Groen T, Wyss JM, Nagy TR, Kesterson RA, Yoder BK.** Disruption of intraflagellar transport in adult mice leads to obesity and slow-onset cystic kidney disease. *Curr Biol* 17: 1586–1594, 2007.
9. **Driscoll JA, Bhalla S, Liapis H, Ibricevic A, Brody SL.** Autosomal dominant polycystic kidney disease is associated with an increased prevalence of radiographic bronchiectasis. *Chest* 133: 1181–1188, 2008.
10. **Evander E, Arborelius M Jr, Jonson B, Simonsson BG, Svensson G.** Lung function and bronchial reactivity in six patients with immotile cilia syndrome. *Eur J Respir Dis Suppl* 127: 137–143, 1983.
11. **Fisher JT, Zhang Y, Engelhardt JF.** Comparative biology of cystic fibrosis animal models. *Methods Mol Biol* 742: 311–334, 2011.
12. **Gupta K, Joshi K, Jindal SK, Rayat CS.** Spectrum of pulmonary adenocarcinoma with ultrastructural correlation: an autopsy study from northern India. *Indian J Pathol Microbiol* 51: 329–336, 2008.
13. **Hayashi S, McMahon AP.** Efficient recombination in diverse tissues by a tamoxifen-inducible form of Cre: a tool for temporally regulated gene activation/inactivation in the mouse. *Dev Biol* 244: 305–318, 2002.
14. **Haycraft CJ, Zhang Q, Song B, Jackson WS, Detloff PJ, Serra R, Yoder BK.** Intraflagellar transport is essential for endochondral bone formation. *Development* 134: 307–316, 2007.
15. **Hewitt M, Creel A, Estell K, Davis IC, Schwiebert LM.** Acute exercise decreases airway inflammation, but not responsiveness, in an allergic asthma model. *Am J Respir Cell Mol Biol* 40: 83–89, 2009.
16. **Hewitt M, Estell K, Davis IC, Schwiebert LM.** Repeated bouts of moderate-intensity aerobic exercise reduce airway reactivity in a murine asthma model. *Am J Respir Cell Mol Biol* 42: 243–249, 2010.
17. **Horsfield K, Kemp W, Phillips S.** Daimeters of Arteries, Veins, and Airways in Isolated Dog Lung. *Anat Rec* 216: 392–395, 1986.
18. **Jain R, Javidan-Nejad C, Alexander-Brett J, Horani A, Cabellon MC, Walter MJ, Brody SL.** Sensory functions of motile cilia and implication for bronchiectasis. *Front Biosci (Schol Ed)* 4: 1088–1098, 2012.
19. **Jain R, Pan J, Driscoll JA, Wisner JW, Huang T, Gunsten SP, You Y, Brody SL.** Temporal relationship between primary and motile ciliogenesis in airway epithelial cells. *Am J Respir Cell Mol Biol* 43: 731–739, 2010.
20. **Kang EY.** Large airway diseases. *J Thorac Imaging* 26: 249–262, 2011.
21. **Koh YY, Lee MH, Sun YH, Sung KW, Chae JH.** Effect of roxithromycin on airway responsiveness in children with bronchiectasis: a double-blind, placebo-controlled study. *Eur Respir J* 10: 994–999, 1997.
22. **Lorenzo IM, Liedtke W, Sanderson MJ, Valverde MA.** TRPV4 channel participates in receptor-operated calcium entry and ciliary beat frequency regulation in mouse airway epithelial cells. *Proc Natl Acad Sci USA* 105: 12611–12616, 2008.
23. **Love D, Li FQ, Burke MC, Cyge B, Ohmitsu M, Cabello J, Larson JE, Brody SL, Cohen JC, Takemaru K.** Altered lung morphogenesis, epithelial cell differentiation and mechanics in mice deficient in the Wnt/beta-catenin antagonist Chibby. *PLoS One* 5: e13600, 2010.
24. **Lu CJ, Du H, Wu J, Jansen DA, Jordan KL, Xu N, Sieck GC, Qian Q.** Non-random distribution and sensory functions of primary cilia in vascular smooth muscle cells. *Kidney Blood Press Res* 31: 171–184, 2008.
25. **Mason SB, Liang Y, Sinders RM, Miller CA, Eggleston-Gulyas T, Crisler-Roberts R, Harris PC, Gattone VH 2nd.** Disease stage characterization of hepatorenal fibrocystic pathology in the PCK rat model of ARPKD. *Anat Rec (Hoboken)* 293: 1279–1288, 2010.
26. **Ostrowski LE, Yin W, Rogers TD, Busalacchi KB, Chua M, O'Neal WK, Grubb BR.** Conditional deletion of dnaic1 in a murine model of primary ciliary dyskinesia causes chronic rhinosinusitis. *Am J Respir Cell Mol Biol* 43: 55–63, 2010.
27. **Peao MN, Aguas AP, de Sa CM, Grande NR.** Anatomy of Clara cell secretion: surface changes observed by scanning electron microscopy. *J Anat* 182: 377–388, 1993.
28. **Reynolds SD, Malkinson AM.** Clara cell: progenitor for the bronchiolar epithelium. *Int J Biochem Cell Biol* 42: 1–4, 2010.
29. **Reynolds SD, Brechbuhl HM, Smith MK, Smith RW, Ghosh M.** Lung epithelial healing: a modified seed and soil concept. *Proc Am Thorac Soc* 9: 27–37, 2012.
30. **Rock JR, Hogan BL.** Epithelial progenitor cells in lung development, maintenance, repair, and disease. *Annu Rev Cell Dev Biol* 27: 493–512, 2011.
31. **Sauer B.** Inducible gene targeting in mice using the Cre/lox system. *Methods* 14: 381–392, 1998.
32. **Schmid A, Salathe M.** Ciliary beat co-ordination by calcium. *Biol Cell* 103: 159–169, 2011.
33. **Shah AS, Ben-Shahar Y, Moninger TO, Kline JN, Welsh MJ.** Motile cilia of human airway epithelia are chemosensory. *Science* 325: 1131–1134, 2009.
34. **Taulman PD, Haycraft CJ, Balkovetz DF, Yoder BK.** Polaris, a protein involved in left-right axis patterning, localizes to basal bodies and cilia. *Mol Biol Cell* 12: 589–599, 2001.
35. **Voronina VA, Takemaru K, Treuting P, Love D, Grubb BR, Hajjar AM, Adams A, Li FQ, Moon RT.** Inactivation of Chibby affects function of motile airway cilia. *J Cell Biol* 185: 225–233, 2009.
36. **Ware SM, Aygun MG, Hildebrandt F.** Spectrum of clinical diseases caused by disorders of primary cilia. *Proc Am Thorac Soc* 8: 444–450, 2011.
37. **Wong AP, Keating A, Waddell TK.** Airway regeneration: the role of the Clara cell secretory protein and the cells that express it. *Cytotherapy* 11: 676–687, 2009.
38. **Wu J, Du H, Wang X, Mei C, Sieck GC, Qian Q.** Characterization of primary cilia in human airway smooth muscle cells. *Chest* 136: 561–570, 2009.
39. **Wyatt TA, Forget MA, Adams JM, Sisson JH.** Both cAMP and cGMP are required for maximal ciliary beat stimulation in a cell-free model of bovine ciliary axonemes. *Am J Physiol Lung Cell Mol Physiol* 288: L546–L551, 2005.